overweighting at large $|F_o|$ and small $(\sin\theta)/\lambda$. Weights were subsequently adjusted to reduce the variation in $\langle w|F_o| - |F_c|)^2\rangle$ as a function of these variables.

The hydrogen positions were calculated by assuming ideal geometries with the C–H bond distance set to 1.0 Å. The least-squares procedure converged to a conventional residual index of $R = \sum||F_o| - |F_c||/\sum|F_o| = 0.108$ and a weighted residual index of $R_w = [\sum w(|F_o| - |F_c|)^2/\sum w|F_c|^2]^{1/2} = 0.110$. The atomic scattering factors were those from ref 29.

The final positional and thermal parameters are listed in Table VI for atoms in the $Pt_2(\mu\text{-dppm})_2$ ring, while bond angles and lengths for atoms other than phenyl carbons are listed in Tables I and VII, respectively. The final positional and thermal parameters for phenyl carbons and hydrogen atoms and anisotropic thermal parameters as well as bond distances and angles of carbons within the phenyl rings are found in the supplementary material accompanied by least-squares planes of these rings, selected torsional angles for atoms in the $Pt_2(\mu\text{-dppm})_2$ ring, and an ORTEP drawing of the disordered phenyl groups.

Acknowledgment. This work, based in part on the Ph.D. thesis of R.J.B., was supported by the U.S. Department of Energy, Office of Basic Energy Sciences, Division of Chemical Sciences, under Contract W-7405-Eng-82. We are grateful to Professors J. G. Verkade and W. S. Trahanovsky for useful discussions. The Nicolet NT-300 NMR spectrometer was purchased in part with funds from a grant (No. CHE-3209709) from the National Science Foundation to the Department of Chemistry at Iowa State University.

Registry No. $(Cl\text{--}PPh_3)(PF_6)\cdot 3C_6H_6$, 100230-50-0; (Cl--Cl), 61250-65-5; $(I\text{--}PPh_3)^+$, 100230-51-1; (I--I), 61289-07-4; $(Ph_3P\text{--}PPh_3)^{2+}$, 69215-88-9; $(Cl\text{--}dppm)^+$, 100230-52-2.

Supplementary Material Available: Tables reporting full structural parameters and an ORTEP drawing of the disordered phenyl groups (21 pages). Ordering information is given on any current masthead page.

---

(29) "International Tables for X-ray Crystallography"; Kynoch Press: Birmingham, England, 1974; Vol. IV, pp 71–79. "International Tables for X-ray Crystallography"; Kynoch Press: Birmingham, England, 1962; Vol. IV, pp 215–216.

Contribution from the Department of Chemistry and Laboratory for Molecular Structure and Bonding,
Texas A&M University, College Station, Texas 77843

Tetramethyldiplatinum(III) (Pt–Pt) Complexes with 2-Hydroxypyridinato Bridging Ligands

Daniel P. Bancroft, F. Albert Cotton,* Larry R. Falvello, and Willi Schwotzer

Received September 24, 1985

Four compounds of the type $[Pt_2(CH_3)_4(\mu\text{-xhp})_2L_n]$, in which xhp^- is one of the anions 2-oxypyridine (hp^-), 2-oxy-6-fluoropyridine (fhp^-), 2-oxy-6-chloropyridine (chp^-), or 2-oxy-6-methylpyridine (mhp^-), have been prepared and characterized. The general preparative method is to react $[Pt(CH_3)_2(\mu\text{-}C_2H_5)_2S]_2$ (**1**) with the appropriate silver salt. The compound $[Pt_2(CH_3)_4(O_2CCH_3)_2(py)_2]$ (**2**) has also been prepared and structurally characterized, and the crystal structure of the starting material, **1**, has been determined. For **1**, a centrosymmetric structure, in which $(C_2H_5)_2S$ ligands bridge $Pt(CH_3)_2$ units to give a planar four-membered ring with $\angle Pt\text{–}S\text{–}Pt = 100.1\ (1)^\circ$ and $\angle S\text{–}Pt\text{–}S = 79.9\ (1)^\circ$, is found. The crystals are triclinic ($P\bar{1}$), with $a = 7.481\ (5)$ Å, $b = 9.114\ (3)$ Å, $c = 9.163\ (5)$ Å, $\alpha = 90.60\ (4)^\circ$, $\beta = 113.62\ (4)^\circ$, $\gamma = 93.41\ (4)^\circ$, $V = 571.0\ (5)$ Å^3, and $Z = 1$. For compound **2**, which forms orthorhombic crystals ($Ibca$) with $a = 16.007\ (6)$ Å, $b = 17.443\ (4)$ Å, $c = 15.051\ (5)$ Å, $V = 4202\ (2)$ Å^3, and $Z = 8$, a Pt–Pt distance of 2.529 (1) Å is found. Compound **3**, $[Pt_2(CH_3)_4(hp)_2(py)_2]\cdot 2CHCl_3$, forms orthorhombic crystals ($P2_12_12_1$), with $a = 14.174\ (4)$ Å, $b = 24.485\ (8)$ Å, $c = 9.820\ (2)$ Å, $V = 3408\ (2)$ Å^3, and $Z = 4$, and has a Pt–Pt distance of 2.550 (1) Å. Compound **4**, $[Pt_2(CH_3)_4(fhp)_2(py)_2]\cdot 0.17C_6H_6$, forms trigonal crystals ($R\bar{3}$), with $a = b = 32.767\ [17]$ Å, $c = 12.629\ (2)$ Å, $V = 11\,743\ (14)$ Å^3, and $Z = 18$, and has a Pt–Pt distance of 2.551 (2) Å. Compound **5**, $[Pt_2(CH_3)_4(chp)_2(py)]$, which forms triclinic crystals ($P\bar{1}$) with $a = 8.839\ (4)$ Å, $b = 9.475\ (4)$ Å, $c = 13.109\ (6)$ Å, $\alpha = 92.00\ (3)^\circ$, $\beta = 90.61\ (4)^\circ$, $\gamma = 96.38\ (4)^\circ$, $V = 1090\ (2)$ Å^3, and $Z = 2$, has a Pt–Pt distance of 2.545 (1) Å. Lastly, compound **6**, $[Pt_2(CH_3)_4(mhp)_2(py)]$, forms triclinic crystals ($P\bar{1}$), with $a = 8.005\ (1)$ Å, $b = 8.774\ (2)$ Å, $c = 15.970\ (3)$ Å, $\alpha = 94.16\ (2)^\circ$, $\beta = 90.27\ (2)^\circ$, $\gamma = 100.63\ (1)^\circ$, $V = 1099.2\ (7)$ Å^3, and $Z = 2$, and has a Pt–Pt distance of 2.543 (1) Å. In complexes **3**–**6**, the geometry is dependent upon the size of the substituent on the pyridine ring. If the substituent is relatively small (i.e., H or F), the complex contains a nonpolar arrangement of bridging ligands and both axial positions are occupied. When the substituent is large (i.e., Cl or CH_3), a polar arrangement of the bridging ligands is observed and one of the axial sites is vacant due to steric interference from the ligand substituent. This results in complexes in which one platinum atom is formally 5-coordinate and the other platinum atom is formally 6-coordinate.

Introduction

Although the earliest reports of diplatinum(III) chemistry appeared in the first decade of this century,[1] it has only been within the last 12 years that a systematic development of such chemistry has taken place.[2,3] One class of these compounds are those of the type $[Pt_2R_4(O_2CR')_2L_2]$, where R = Ph and Me, R′ = one of a variety of organic radicals, and L = one of a variety of donors. These were first prepared and described in 1976 and 1977 by Vrieze and co-workers,[4,5] who synthesized them from the $[PtR_2(\mu\text{-}Et_2S)]_2$ starting materials[6,7] by the following type of reaction sequence:

$$[Pt_2(CH_3)_4(R_2S)_2] + 2Ag(O_2CR') \rightarrow [Pt_2(CH_3)_4(O_2CR')_2(R_2S)_2] + 2Ag^0$$

$$[Pt_2(CH_3)_4(O_2CR')_2(R_2S)_2] + \text{excess pyridine} \rightarrow [Pt_2(CH_3)_4(O_2CR')_2(py)_2] + 2R_2S$$

Only one of these compounds, $[Pt_2(CH_3)_4(O_2CCF_3)_2(4\text{-}MeC_5H_4N)_2]$, has been structurally characterized by X-ray crystallography.[8]

---

(1) (a) Blondel, M. *Ann. Chim. Phys.* **1905**, *8*, 110. (b) Wohler, L.; Frey, W. *Z. Elektrochem.* **1909**, *15*, 132. (c) Delephine, M. *C. R. Hebd. Seances Acad. Sci.* **1910**, *150*, 104.

(2) O'Halloran, T. V.; Lippard, S. J. *Isr. J. Chem.* **1985**, *25*, 130.

(3) Cotton, F. A.; Walton, R. A. *Struct. Bonding*, in press.

(4) Kuyper, J.; Vrieze, K. *Transition Met. Chem.* (*Weinheim, Ger.*) **1976**, *1*, 208.

(5) Steele, B. R.; Vrieze, K. *Transition Met. Chem.* (*Weinheim, Ger.*) **1977**, *2*, 169.

(6) Kuyper, J.; van der Laan, R.; Jeanneaus, F.; Vrieze, K. *Transition Met. Chem.* (*Weinheim, Ger.*) **1976**, *1*, 199.

(7) Steele, B. R.; Vrieze, K. *Transition Met. Chem.* (*Weinheim, Ger.*) **1977**, *2*, 140.

0020-1669/86/1325-0763$01.50/0

Using a variation of Vrieze's method, we have been able to prepare a new series of novel and interesting Pt(III) complexes. The complexes contain hydroxypyridine derivatives, which are well-known to give compounds with novel coordination geometries, as bridging ligands. The coordination geometry of the resultant complex is dependent upon the size of the substituent on the pyridine ring. If the substituent is relatively small (i.e., H or F), the complex contains a nonpolar arrangement of bridging ligands and both axial positions are occupied. When the substituent is large (i.e., Cl or CH_3), a polar arrangement of the bridging ligands is observed and one of the axial sites is vacant due to steric interference from the ligand substituent. This results in complexes in which one platinum atom is formally 5-coordinate and the other platinum atom is formally 6-coordinate.

The complexes can readily be prepared by the following reaction sequence:

$$[Pt_2(CH_3)_4(R_2S)_2] + 2Ag(xhp) \rightarrow [Pt_2(CH_3)_4(xhp)_2(R_2S)_n] + 2Ag^0$$

$$[Pt_2(CH_3)_4(xhp)_2(R_2S)_n] + \text{excess pyridine} \rightarrow [Pt_2(CH_3)_4(xhp)_2(py)_n] + nR_2S$$

where $R = C_2H_5$, x = H, F, Cl, or CH_3, and $n = 1$ or 2, depending upon the size of x. The complexes formed are typically very soluble in most organic solvents and are stable both in the solid state and in solution for long periods of time.

In this paper we present the complete synthetic details and X-ray structural characterization of these new complexes. In addition, we have structurally characterized the very useful starting material $[Pt_2(CH_3)_4((C_2H_5)_2S)_2]$, as well as $[Pt_2(CH_3)_4(O_2CCH_3)_2(py)_2]$ for comparative purposes. A discussion of the effects of the coordination geometry of the ligands upon the structures is also included.

Experimental Section

Throughout this paper the following abbreviations will be used: Hhp = 2-hydroxypyridine (also known as α-pyridone); Hchp = 2-hydroxy-6-chloropyridine; Hmhp = 2-hydroxy-6-methylpyridine; Hfhp = 2-hydroxy-6-fluoropyridine.

Preparation of Ag Salts. Silver acetate was purchased from Aldrich Chemical Co. and was used without further purification. Stoichiometric amounts of $AgNO_3$ solution were added to aqueous solutions of the sodium salts of the ligands, which were prepared previously by the addition of NaOMe in methanol to the respective ligands. The Ag salts precipitated immediately in all cases and were subsequently filtered, washed with several portions of water, ethanol, and ether, and air-dried. The Ag salts were typically off-white and moderately light-sensitive.

Preparation of $[Pt_2(CH_3)_4((C_2H_5)_2S)_2]$ (1). $[Pt_2(CH_3)_4((C_2H_5)_2S)_2]$ was prepared by a modification of the previously published method.[4] MeLi was used to methylate *cis*-$PtCl_2((C_2H_5)_2S)_2$ rather than Me_2Mg as suggested by the authors. The complex was recrystallized from $CHCl_3$ prior to use to remove an impurity present after the initial preparation. Crystals of $[Pt_2(CH_3)_4((C_2H_5)_2S)_2]\cdot C_6H_6$ were grown from a benzene solution at 5 °C over the course of several days.

Preparation of $[Pt_2(CH_3)_4(O_2CCH_3)_2(py)_2]$ (2). The complex was prepared by the previously published method of Vrieze et al.[5] A suspension of $[Pt_2(CH_3)_4((C_2H_5)_2S)_2]$ (0.50 g, 0.79 mmol) and $Ag(O_2CCH_3)$ (0.26 g, 1.58 mmol) in 40 mL of dry benzene was stirred at room temperature for 6 h. The mixture was filtered through Celite to remove colloidal Ag^0 and the solvent removed under vacuum. An excess of pyridine (ca. 20 mL) was added, and the golden yellow solution was stirred for several hours and subsequently filtered to remove a small amount of Ag^0. The complex was very difficult to crystallize; however, after several attempts, crystals suitable for X-ray diffraction were grown by slow evaporation of an ethanol solution.

Preparation of $[Pt_2(CH_3)_4(hp)_2(py)_2]$ (3). A suspension of $[Pt_2(CH_3)_4((C_2H_5)_2S)_2]$ (0.20 g, 0.32 mmol) and Ag(hp) (0.13 g, 0.64 mmol) in 40 mL of dry benzene was stirred at room temperature for 48 h. The initially white suspension gradually darkened and eventually appeared almost black. The colloidal Ag^0 was removed by vacuum filtration through Celite, and the remaining golden yellow solution was evaporated to dryness under vacuum. An excess of pyridine (ca. 10 mL) was added, and the solution was subsequently filtered after being stirred at room temperature for several hours. The excess pyridine was then removed in vacuum, and the yellow oil remaining was dissolved in dry $CHCl_3$ (ca. 10 mL). The volume was then reduced to approximately 1 mL, and the yellow solution was slowly cooled to −15 °C. Large yellow crystals suitable for X-ray diffraction formed after about 3 h.

Preparation of $[Pt_2(CH_3)_4(fhp)_2(py)_2]$ (4). A suspension of $[Pt_2(CH_3)_4((C_2H_5)_2S)_2]$ (0.12 g, 0.19 mmol) and Ag(fhp) (0.084 g, 0.38 mmol) in 30 mL of dry benzene was stirred for 24 h. The initially white suspension gradually changed to green and after about 12 h appeared black. The colloidal Ag^0 was removed by vacuum filtration through Celite, and the remaining orange-yellow solution was evaporated to dryness under vacuum. An excess of pyridine (ca. 10 mL) was added and the solution filtered after being stirred at room temperature for several hours. Greenish yellow crystals were grown by slow evaporation of a 1:1 mixture of benzene and pyridine in air.

Preparation of $[Pt_2(CH_3)_4(chp)_2(py)]$ (5). A suspension of $[Pt_2(CH_3)_4((C_2H_5)_2S)_2]$ (0.10 g, 0.16 mmol) and Ag(chp) (0.075 g, 0.32 mmol) in 25 mL of dry benzene was stirred at room temperature for 48 h. The suspension, which was initially white, gradually changed to blue-green and eventually appeared black. The colloidal Ag^0 was removed by vacuum filtration through Celite, and the remaining golden yellow solution was evaporated to dryness under vacuum. An excess of pyridine was then added (ca. 10 mL) and the solution stirred for several hours and subsequently filtered. The volume was then reduced to approximately 2 mL and the solution cooled to 5 °C. Orange crystals, suitable for X-ray diffraction, formed after about 1 week.

Preparation of $[Pt_2(CH_3)_4(mhp)_2(py)]$ (6). A suspension of $[Pt_2(CH_3)_4((C_2H_5)_2S)_2]$ (0.20 g, 0.32 mmol) and Ag(mhp) (0.14 g, 0.64 mmol) in 40 mL of dry benzene was stirred at room temperature for 72 h. The suspension, which was initially white, gradually changed to a brown-black color. The colloidal Ag^0 was removed by vacuum filtration through Celite. An excess of pyridine (ca. 10 mL) was added to the orange solution, which was subsequently stirred, filtered, and evaporated to about 4 mL under vacuum. Orange-red crystals suitable for X-ray diffraction were grown by slow evaporation in air.

X-ray Crystallography

$[Pt_2(CH_3)_4((C_2H_5)_2S)_2]\cdot C_6H_6$ (1). A crystal with dimensions 0.3 × 0.4 × 0.4 mm was quickly coated with epoxy cement and mounted on top of a glass fiber. A Syntex P3 diffractometer equipped with graphite-monochromated Mo Kα (λ = 0.71073 Å) radiation was used to collect 2163 unique reflections of which 1763 had $I > 3\sigma(I)$. Lorentz, polarization, and absorption corrections were applied. Relevant crystal parameters and data are given in Table I.

Preliminary examination of the crystal showed it to be of triclinic symmetry, and the space group was assumed to be $P\bar{1}$. The platinum atom position was obtained from the Patterson function. The molecule resides on the inversion center at the origin. The remaining non-hydrogen atoms were revealed by alternating difference Fourier maps and least-squares cycles. No attempt was made to locate the hydrogen atom positions. In addition to the Pt(II) dimer, the structure contains a benzene molecule as a solvent of crystallization, which resides on an inversion center at ($^1/_2$, $^1/_2$, 0). Full-matrix least-squares refinement converged to final residuals of $R = 0.047$ and $R_w = 0.065$. Expressions for R and R_w are included in Table I. All atoms were refined with anisotropic thermal parameters. The largest peak in the final difference map was 2.304 e/Å^3 and was located near the platinum atom position.

$[Pt_2(CH_3)_4(O_2CCH_3)_2(py)_2]$ (2). A crystal with dimensions 0.3 × 0.4 × 0.4 mm was coated with epoxy cement and mounted on top of a glass fiber. An Enraf-Nonius CAD-4 diffractometer equipped with graphite-monochromated Mo Kα (λ = 0.71073 Å) radiation was used to collect 1209 unique reflections of which 1070 had $I > 3\sigma(I)$. Lorentz, polarization, and absorption corrections were applied. Relevant crystal parameters and data are given in Table I.

Preliminary examination of the data showed the unit cell to be body-centered orthorhombic. The space group was uniquely determined by the systematic absences to be *Ibca*. Successful refinement confirmed that the space group was correct. The platinum atom position was located from the Patterson map. Alternating difference Fourier maps and least-squares cycles revealed the remaining non-hydrogen atoms. All atoms were refined with anisotropic thermal parameters. Full-matrix least-squares refinement converged to final residuals of $R = 0.034$ and $R_w = 0.044$. The largest peak in the final difference map was *ca.* 0.9 e/Å^3 and was located near the platinum atom position.

$[Pt(CH_3)_4(hp)_2(py)_2]\cdot 2CHCl_3$ (3). A crystal with dimensions 0.5 × 0.6 × 0.5 mm was coated with epoxy cement and mounted on top of a glass fiber. A Syntex P$\bar{1}$ four-circle diffractometer equipped with graphite-monochromated Mo Kα (λ = 0.71073 Å) radiation was used to collect 2496 unique reflections of which 2274 had $I > 3\sigma(I)$. Lorentz, polarization, and absorption corrections (by the ψ-scan method) were applied. The original absorption correction was determined to be inad-

---

(8) Schagen, J. D.; Overbeek, A. R.; Schenk, H. *Inorg. Chem.* **1978**, *17*, 1938.

Table I. Crystal Data

formula	$[Pt_2(CH_3)_4((C_2H_5)_2S)_2]\cdot C_6H_6$ (**1**)	$[Pt_2(CH_3)_4(O_2CCH_3)_2(py)_2]$ (**2**)	$[Pt_2(CH_3)_4(hp)_2(py)_2]\cdot 2CHCl_3$ (**3**)	$[Pt_2(CH_3)_4(fhp)_2(py)_2]\cdot 0.17C_6H_6$ (**4**)	$[Pt_2(CH_3)_4(chp)_2(py)]$ (**5**)	$[Pt_2(CH_3)_4(mhp)_2(py)]$ (**6**)
fw	708.81	726.61	1067.47	832.69	785.50	745.66
space group	$P\bar{1}$	*Ibca*	$P2_12_12_1$	$R\bar{3}$	$P\bar{1}$	$P\bar{1}$
syst abs	none	hkl ($h + k + l = 2N + 1$), $h0l$ ($l = 2n + 1$), $0kl$ ($k = 2n + 1$), $hk0$ ($h = 2n + 1$)	$h00$ ($h = 2n + 1$), $0k0$ ($k = 2n + 1$), $00l$ ($l = 2n + 1$)	hkl ($-h + k + 1 \neq 3n$)	none	none
a, Å	7.481 (5)	16.007 (6)	14.174 (4)	32.767 [17]	8.839 (4)	8.005 (1)
b, Å	9.114 (3)	17.443 (4)	24.485 (8)	32.767 [17]	9.475 (4)	8.774 (2)
c, Å	9.163 (5)	15.051 (5)	9.820 (2)	12.629 (2)	13.109 (6)	15.970 (3)
α, deg	90.60 (4)	90.00	90.00	90.00	92.00 (3)	94.16 (2)
β, deg	113.62 (4)	90.00	90.00	90.00	90.61 (4)	90.27 (2)
γ, deg	93.41 (4)	90.00	90.00	120.00	96.38 (4)	100.63 (1)
V, Å^3	571.0 (5)	4202.3 (23)	3407.8 (16)	11743 (14)	1090.3 (15)	1099.2 (7)
Z	1	8	4	18	2	2
d_{calcd}, g/cm^3	2.061	2.297	2.080	2.119	2.395	2.253
cryst size, mm	0.3 × 0.4 × 0.4	0.3 × 0.4 × 0.4	0.5 × 0.6 × 0.5	0.35 × 0.4 × 0.4	0.5 × 0.5 × 0.4	0.3 × 0.4 × 0.5
μ(Mo Kα), cm^{-1}	125.3	134.65	87.99	108.63	132.2	128.67
data collcn instrum	P3	CAD-4	P3	CAD-4	CAD-4	CAD-4
radiation (monochromated in incident beam)	Mo Kα (λ = 0.71073 Å)	Mo Kα (λ = 0.71073 Å)	Mo Kα (λ = 0.71073 Å)	Mo Kα (λ = 0.71073 Å)	Mo Kα (λ = 0.71073 Å)	Mo Kα (λ = 0.71073 Å)
no. of orientation reflcns; range (2θ), deg	15; 4.48–23.25	25; 6.772–33.092	25; 20.90–29.69	25; 6.06–29.76	25; 20.89–33.75	25; 17.92–30.08
temp, °C	25	25	25	25	25	25
scan method	θ–2θ	θ–2θ	θ–2θ	θ–2θ	θ–2θ	θ–2θ
data collcn range (2θ) deg	4.0–50.0	4.0–50.0	4.0–45.0	4.0–45.0	4.0–50.0	4.0–50.0
no. of unique data; total with $F_o^2 > 3\sigma(F_o^2)$	2163; 1763	1209; 1070	2496; 2274	2290; 1492	3051; 2058	3169; 2660
no. of params refined	100	118	356	292	253	253
transmissn factors: max, min	99.99%, 40.10%	99.33%, 91.70%	130.7%, 76.74%	99.91%, 93.63%	99.72%, 78.54%	99.74%, 36.73%
R^a	0.04759	0.03406	0.03881	0.03450	0.04742	0.03663
R_w^b	0.06494	0.04422	0.05222	0.05102	0.05892	0.04763
quality of fit indicator^c	1.523	1.008	1.229	1.127	1.760	1.368
largest shift/esd, final cycle	0.04	0.03	0.09	0.29	0.42	0.02
largest peak, e/Å^3	2.304	0.921	0.936	0.897	2.480	2.083

[a] $R = \sum \lVert F_o\rvert - \lvert F_c \rVert / \sum \lvert F_o \rvert$. [b] $R_w = [\sum w(\lvert F_o\rvert - \lvert F_c\rvert)^2/\sum w\lvert F_o\rvert^2]^{1/2}$; $w = 1/\sigma^2(\lvert F_o\rvert)$. [c] Quality of fit $= [\sum w(\lvert F_o\rvert - \lvert F_c\rvert)^2/(N_{observns} - N_{params})]^{1/2}$.

Table II. Positional and Thermal Parameters and Their Esd's for $[Pt_2(CH_3)_4((C_2H_5)_2S)_2]\cdot C_6H_6$[a]

atom	*x*	*y*	*z*	*B*, Å^2
Pt(1)	0.06835 (6)	0.14173 (5)	0.39220 (5)	1.912 (9)
S(1)	−0.0528 (5)	−0.1065 (3)	0.3590 (4)	2.26 (6)
C(1)	0.076 (3)	0.154 (2)	0.169 (2)	4.6 (4)
C(2)	0.175 (2)	0.358 (2)	0.438 (2)	3.8 (3)
C(3)	0.285 (2)	0.146 (2)	0.810 (2)	3.4 (3)
C(4)	0.094 (2)	−0.233 (2)	0.308 (2)	3.6 (3)
C(5)	0.438 (3)	0.055 (3)	0.800 (2)	5.2 (5)
C(6)	0.296 (2)	−0.236 (2)	0.442 (2)	5.0 (4)
C(7)	0.479 (3)	0.445 (2)	1.135 (2)	5.2 (5)
C(8)	0.363 (3)	0.585 (2)	0.892 (2)	4.7 (5)
C(9)	0.338 (3)	0.528 (3)	1.029 (3)	5.9 (6)

[a] The isotropic equivalent thermal parameters of the anisotropically refined atoms are defined as $^4/_3[a^2\beta_{11} + b^2\beta_{22} + c^2\beta_{33} + ab(\cos\gamma)\beta_{12} + ac(\cos\beta)\beta_{13} + bc(\cos\alpha)\beta_{23}]$.

Table III. Interatomic Distances and Their Esd's in Angstroms for $[Pt_2(CH_3)_4((C_2H_5)_2S)_2]\cdot C_6H_6$[a]

atom 1	atom 2	dist	atom 1	atom 2	dist
Pt(1)	Pt(1)	3.610 (1)	S(1)	C(4)	1.819 (12)
Pt(1)	S(1)	2.356 (3)	C(3)	C(5)	1.48 (2)
Pt(1)	S(1)	2.353 (3)	C(4)	C(6)	1.53 (2)
Pt(1)	C(1)	2.072 (15)	C(7)	C(9)	1.39 (2)
Pt(1)	C(2)	2.052 (13)	C(8)	C(9)	1.43 (3)
S(1)	C(3)	1.822 (12)			

[a] Numbers in parentheses are estimated standard deviations in the least significant digits.

equate, and an additional empirical correction was applied (DIFABS). Relevant crystal parameters and data are given in Table I.

Preliminary examination showed the crystal to be of orthorhombic symmetry. The space group was determined to be $P2_12_12_1$ from the systematic absences, and the structure was successfully refined in this space group. The heavy atom positions were obtained from the direct-methods program MULTAN 11/82. Subsequent alternating difference Fourier maps and least-squares cycles revealed the remaining non-hydrogen atoms as well as two $CHCl_3$ solvent molecules. No attempts were made to locate the hydrogen atom positions. With the exception of carbon atom C(10), all atoms were refined with anisotropic thermal parameters. Full-matrix least-squares refinement converged to final residuals of $R = 0.039$ and $R_w = 0.052$. Refinement of the other enantiomer gave residuals of $R = 0.047$ and $R_w = 0.061$. The largest peak in the final difference map was ca. 0.9 e/Å^3.

$[Pt_2(CH_3)_4(fhp)_2(py)_2]\cdot 0.17C_6H_6$ (4). A crystal with dimensions of 0.4 × 0.3 × 0.3 mm was mounted on top of a glass fiber with epoxy cement. An Enraf-Nonius CAD-4 diffractometer equipped with graphite-monochromated Mo Kα (λ = 0.71073 Å) radiation was used to collect 2290 reflections of which 1492 had $I > 3\sigma(I)$. Lorentz, polarization, and absorption corrections (by the ψ-scan method) were applied. Unit cell parameters and other pertinent crystal data are given in Table I.

Preliminary examination of the crystal showed it to be of trigonal symmetry with the space group being either $R3$ or $R\bar{3}$. The centrosymmetric space group, $R\bar{3}$, was confirmed by successful refinement. Intensity data were collected on the equivalent, alternative setting of the hexagonal axes. The heavy atom positions were obtained by the direct-methods program MULTAN 11/82. Alternating difference Fourier maps and least-squares cycles revealed the remaining nonhydrogen atoms. The structure also contains a disordered benzene molecule which lies about a $\bar{3}$ axis and has a multiplicity of 3. Full-matrix least-squares refinement converged to final residuals of $R = 0.034$ and $R_w = 0.051$. The largest peak in the final difference map was ca. 0.9 e/Å^3 and was located close to one of the fluorine atoms.

$[Pt_2(CH_3)_4(chp)_2(py)]$ (5). A crystal with dimensions 0.5 × 0.5 × 0.4 mm was coated with epoxy cement and mounted on top of a glass fiber.

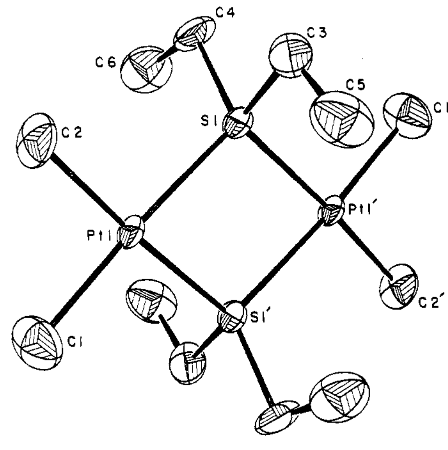

Figure 1. ORTEP view of $[Pt_2(CH_3)_4((C_2H_5)_2S)_2]$.

An Enraf-Nonius CAD-4 diffractometer equipped with graphite-monochromated Mo Kα (λ = 0.71073 Å) radiation was used to collect 3051 unique reflections of which 2058 had $I > 3\sigma(I)$. Lorentz, polarization, and absorption corrections (by the ψ-scan method) were applied. Relevant crystal parameters and data are given in Table I.

Preliminary examination of the crystal showed it to be of triclinic symmetry, and the space group was assumed to be $P\bar{1}$. The heavy atom positions were obtained by the direct-methods program MULTAN 11/82. Alternating difference Fourier maps and least-squares cycles revealed the remaining non-hydrogen atoms. No attempt was made to find the hydrogen atoms. Full-matrix least-squares refinement converged to final residuals of $R = 0.047$ and $R_w = 0.059$. The largest peak in the final difference map was ca. 2.5 e/Å^3 and was located close to one of the platinum atoms.

$[Pt_2(CH_3)_4(mhp)_2(py)]$ (6). A crystal with dimensions of 0.4 × 0.4 × 0.5 mm was mounted in a Lindemann glass capillary with epoxy cement. An Enraf-Nonius CAD-4 diffractometer equipped with graphite-monochromated Mo Kα (λ = 0.71073 Å) radiation was used to collect 3169 reflections of which 2660 had $I > 3\sigma(I)$. Lorentz, polarization, and absorption corrections (by the ψ-scan method) were applied. Relevant crystal parameters and data are given in Table I.

Preliminary examination of the crystal showed it to be of triclinic symmetry, and the space group was assumed to be $P\bar{1}$. The heavy atom positions were obtained by the direct-methods program MULTAN 11/82. Alternating difference Fourier maps and least-squares cycles revealed the remaining non-hydrogen atoms. Full-matrix least-squares refinement converged to final residuals of $R = 0.037$ and $R_w = 0.048$. The largest peaks in the final difference map were ca. 2.1 e/Å^3 and were located close to the platinum atoms.

Results

Structure of $[Pt_2(CH_3)_4((C_2H_5)_2S)_2]\cdot C_6H_6$. An ORTEP view of the dinuclear unit is shown in Figure 1. Table II contains the final positional and thermal parameters. Tables III and IV list the bond lengths and angles, respectively.

The structure consists of a cyclic dinuclear Pt(II) molecule with the planar Pt_2S_2 ring having its midpoint on an inversion center. The platinum atoms are bridged by two $(C_2H_5)_2S$ ligands. In addition, each platinum atom is bonded to two methyl groups that are in a cis configuration. Each platinum atom is approximately in a square-planar environment, which is consistent with the platinum atoms being in the +2 oxidation state. The metal–metal separation, which is 3.610 (1) Å, indicates that there is no significant bonding interaction between the platinum atoms. The average Pt–C bond length is 2.062 [10] Å. The diethyl sulfide bridging ligands are symmetrically coordinated through the sulfur atoms with an average Pt–S distance of 2.354 [1] Å. The Pt–S–Pt angles are 100.1 (1)°, and the S–Pt–S angles are 79.9 (1)°,

Table IV. Bond Angles and Their Esd's in Degrees for $[Pt_2(CH_3)_4((C_2H_5)_2S)_2]\cdot C_6H_6$[a]

atom 1	atom 2	atom 3	angle	atom 1	atom 2	atom 3	angle
S(1)	Pt(1)	S(1)	79.9 (1)	S(1)	C(3)	C(5)	111 (1)
Pt(1)	S(1)	Pt(1)	100.1 (1)	S(1)	C(4)	C(6)	111 (1)
C(1)	Pt(1)	C(2)	88.8 (6)	C(7)	C(9)	C(8)	120 (2)
C(3)	S(1)	C(4)	99.0 (7)				

[a] Numbers in parentheses are estimated standard deviations in the least significant digits.

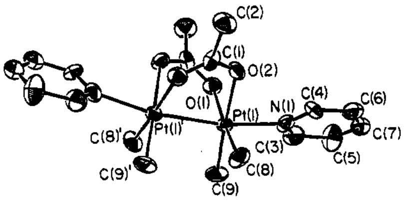

Figure 2. ORTEP view of $[Pt_2(CH_3)_4(O_2CCH_3)_2(py)_2]$.

Table V. Positional and Thermal Parameters and Their Esd's for $[Pt_2(CH_3)_4(O_2CCH_3)_2(py)_2]^a$

atom	*x*	*y*	*z*	*B*, Å^2
Pt(1)	0.20925 (3)	0.14690 (3)	0.07202 (3)	2.180 (8)
O(1)	0.6209 (5)	0.4270 (5)	0.0001 (6)	3.0 (2)
O(2)	0.7210 (6)	0.4570 (5)	0.1009 (6)	2.9 (2)
N(1)	0.3615 (7)	0.6256 (6)	0.1949 (7)	3.1 (2)
C(1)	0.6497 (7)	0.4672 (8)	0.0624 (8)	2.5 (3)
C(2)	0.599 (1)	0.5341 (9)	0.096 (1)	4.1 (4)
C(3)	0.4440 (9)	0.6464 (9)	0.198 (1)	4.3 (3)
C(4)	0.3257 (8)	0.4078 (7)	0.2351 (9)	2.6 (3)
C(5)	0.4859 (9)	0.360 (1)	0.220 (1)	5.0 (4)
C(6)	0.366 (1)	0.4176 (8)	0.154 (1)	4.2 (4)
C(7)	0.451 (1)	0.3921 (9)	0.149 (1)	4.3 (4)
C(8)	0.7031 (9)	0.2918 (8)	0.143 (1)	3.7 (3)
C(9)	0.353 (1)	0.7485 (8)	0.051 (1)	4.6 (4)

[a] The isotropic equivalent thermal parameters of the anisotropically refined atoms are defined as $^4/_3[a^2\beta_{11} + b^2\beta_{22} + c^2\beta_{33} + ab(\cos\gamma)\beta_{12} + ac(\cos\beta)\beta_{13} + bc(\cos\alpha)\beta_{23}]$.

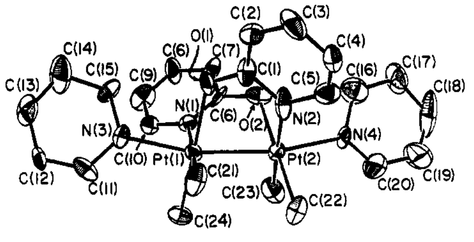

Figure 3. ORTEP view of $[Pt_2(CH_3)_4(hp)_2(py)_2]$.

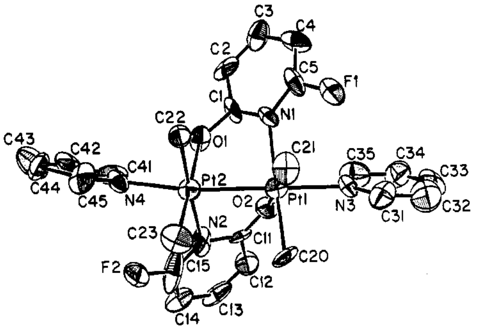

Figure 4. ORTEP view of $[Pt_2(CH_3)_4(fhp)_2(py)_2]$.

indicating that there is at least a slight repulsion between the platinum atoms.

Structure of $[Pt_2(CH_3)_4(O_2CCH_3)_2(py)_2]$. An ORTEP view of the molecule is shown in Figure 2. Table V contains the final positional and thermal parameters. Tables VI and VII list some selected bond lengths and angles, respectively.

The dinuclear Pt(III) molecule lies on a crystallographic 2-fold axis. The Pt–Pt separation is 2.529 (1) Å, which is indicative of a single bond. The platinum atoms are bridged by two acetate ligands with an average Pt–O bond length of 2.186 [20] Å. Each platinum atom is also bonded to two cis methyl groups with an average Pt–C bond length of 2.061 [7] Å. The axial positions are occupied by pyridine molecules with Pt–N distances of 2.200 (11) Å. The Pt–Pt–N_{ax} bond angles are 170.3 (3)°, with the pyridine molecules being bent away from the cis methyl groups. The two, approximately square, *cis*-PtO_2C_2 units have a staggered rotational relationship, with a mean C–Pt–Pt–C torsion angle of ±28.8 [1]°.

Structure of $[Pt_2(CH_3)_4(hp)_2(py)_2]\cdot 2CHCl_3$. An ORTEP view of the dinuclear molecule is shown in Figure 3. Table VIII contains the final positional and thermal parameters. Some selected bond lengths and angles are listed in Tables VI and VII.

The entire dinuclear Pt(III) molecule is the crystallographic asymmetric unit. The Pt–Pt single bond distance is 2.550 (1) Å. The two platinum atoms are bridged in a nonpolar manner by two oppositely directed hydroxypyridine ligands. The average Pt–N_{ligand} and Pt–O_{ligand} bond lengths are 2.14 [1] and 2.164 [15] Å, respectively. The axial positions are occupied by pyridine molecules with an average Pt–N_{ax} bond length of 2.183 [24] Å. The pyridine ligands are bent away from the cis methyl groups

Table VI. Selected Bond Distances and Their Esd's in Angstroms

no.	compd	Pt–Pt	Pt–O	Pt–N	Pt–C	Pt–N_{ax}	O–C	N–C	X–C
2	$[Pt_2(CH_3)_4(O_2CCH_3)_2(py)_2]$	2.529 (1)	2.186 [20]		2.061 [7]	2.200 (11)	1.276 [23]		
3	$[Pt_2(CH_3)_4(hp)_2(py)_2]\cdot 2CHCl_3$	2.550 (1)	2.164 [15]	2.14 [1]	2.06 [2]	2.183 [24]	1.32 [4]	1.38 [4]	
4	$[Pt_2(CH_3)_4(fhp)_2(py)_2]\cdot 0.17C_6H_6$	2.551 (2)	2.14 [3]	2.23 [4]	2.06 [2]	2.20 [1]	1.28 [5]	1.32 [7]	1.38 [3]
5	$[Pt_2(CH_3)_4(chp)_2(py)]$	2.543 (1)	2.144 [14]	2.168 [5]	2.04 [1]	2.060 (11)	1.30 [1]	1.35 [2]	1.74 [1]
6	$[Pt_2(CH_3)_4(mhp)_2(py)]$	2.545 (1)	2.132 [4]	2.158 [4]	2.051 [10]	2.030 (8)	1.294 [5]	1.382 [14]	1.52 [2]

Table VII. Selected Bond Angles and Their Esd's in Degrees

	compounds				
angles	**2**	**3**	**4**	**5**	**6**
Pt–Pt–O	84.8 [1]	84.2 [1]	82.4 [9]	84.9 [13]	83.2 [4]
Pt–Pt–N		84.0 [1]	84.0 [18]	84.2 [6]	84.6 [1]
Pt–Pt–N_{ax}	170.3 (3)	168.1 [17]	167.6 [11]	169.0 (4)	167.2 (2)
Pt–Pt–C	96.0 [10]	98.2 [11]	96.9 [20]	98.0 [13]	98.0 [4]
C–Pt–C	87.8 [6]	88 [2]	88.0 [1]	87.6 [5]	88.2 [18]
Pt–O–C	117.8 [9]	120 [3]	124 [4]	121 [3]	121.7 [4]
Pt–N–C		120 [1]	122 [9]	121 [2]	121 [3]
O–Pt–O	86.6 (3)			87.5 (4)	88.4 (3)
N–Pt–N				89.1 (4)	90.2 (3)
O–Pt–N_{ax}	88.2 [12]	85.4 [10]	85.4 [21]	87.2 [8]	88.0 [1]
C–Pt–N_{ax}	90.8 [10]	89.8 [42]	90 [4]	91.0 [6]	91.0 [7]
cis-O–Pt–C	92.8 [56]	88.5 [1]	90 [1]	92.2 [3]	91.0 [20]
trans-O–Pt–C	175.8 [8]	176.8 [2]	178 [1]	178.2 [13]	178.2 [9]
cis-N–Pt–C		94.1 [28]	94 [2]	91.7 [65]	91.3 [55]
trans-N–Pt–C		175.6 [1]	177 [1]	174.2 [1]	175.0 [12]
O–C–N		119 [3]	118 [4]	118 [2]	118 [1]
C–Pt–Pt–C	28.84 [4]	31 [2]	31.5 [3]	27.2 [1]	31 [2]
O–Pt–Pt–N		26.1 [8]	26.9 [5]	22 [1]	25 [1]
O–Pt–Pt–O	20.92 [4]				

Table VIII. Positional and Thermal Parameters and Their Esd's for $[Pt_2(CH_3)_4(hp)_2(py)_2]\cdot 2CHCl_3$[a]

atom	*x*	*y*	*z*	*B*, Å^2
Pt(1)	0.76916 (5)	0.18562 (3)	0.26227 (6)	2.07 (1)
Pt(2)	0.59393 (5)	0.16743 (3)	0.29955 (7)	2.25 (1)
Cl(1)	0.4345 (8)	0.4479 (4)	0.307 (1)	11.3 (3)
Cl(2)	0.5262 (6)	0.4735 (4)	0.552 (1)	9.2 (3)
Cl(3)	0.5503 (7)	0.3675 (4)	0.443 (2)	11.9 (4)
Cl(4)	0.5922 (7)	0.6192 (4)	0.609 (2)	14.9 (4)
Cl(5)	0.6554 (8)	0.5495 (6)	0.836 (1)	13.5 (4)
Cl(6)	0.7644 (7)	0.5628 (5)	0.597 (1)	11.7 (3)
O(1)	0.7830 (8)	0.0977 (5)	0.288 (1)	2.8 (3)
O(2)	0.605 (1)	0.1208 (5)	0.114 (1)	3.3 (3)
N(1)	0.735 (1)	0.1731 (6)	0.053 (1)	2.3 (3)
N(2)	0.643 (1)	0.0969 (8)	0.408 (2)	3.4 (4)
N(3)	0.920 (1)	0.1827 (6)	0.209 (1)	2.7 (3)
N(4)	0.450 (1)	0.1384 (7)	0.309 (2)	3.1 (3)
C(1)	0.727 (1)	0.0705 (9)	0.367 (2)	3.1 (4)
C(2)	0.752 (2)	0.0228 (8)	0.422 (2)	4.2 (5)
C(3)	0.699 (2)	−0.0023 (9)	0.513 (3)	4.8 (6)
C(4)	0.614 (1)	0.0245 (9)	0.559 (2)	3.9 (5)
C(5)	0.586 (2)	0.0692 (8)	0.503 (2)	3.7 (5)
C(6)	0.667 (1)	0.1379 (8)	0.020 (2)	2.7 (4)
C(7)	0.656 (1)	0.1183 (9)	−0.116 (2)	3.3 (4)
C(8)	0.718 (1)	0.1364 (9)	−0.216 (2)	3.7 (4)
C(9)	0.786 (2)	0.1732 (9)	−0.182 (2)	3.9 (5)
C(10)	0.792 (1)	0.1928 (8)	−0.047 (2)	2.5 (3)*
C(11)	0.985 (1)	0.2266 (8)	0.225 (2)	3.3 (4)
C(12)	1.077 (1)	0.2245 (9)	0.181 (3)	4.7 (5)
C(13)	1.107 (1)	0.176 (1)	0.110 (3)	5.1 (6)
C(14)	1.049 (2)	0.131 (1)	0.092 (3)	6.0 (7)
C(15)	0.951 (2)	0.137 (1)	0.140 (2)	4.6 (5)
C(16)	0.435 (2)	0.084 (1)	0.260 (2)	4.9 (5)
C(17)	0.345 (2)	0.061 (1)	0.266 (3)	5.7 (6)
C(18)	0.267 (2)	0.094 (2)	0.316 (3)	7.8 (8)
C(19)	0.283 (2)	0.144 (1)	0.358 (3)	6.7 (8)
C(20)	0.378 (2)	0.165 (1)	0.357 (3)	4.8 (6)
C(21)	0.811 (2)	0.195 (1)	0.460 (2)	4.2 (5)
C(22)	0.575 (2)	0.217 (1)	0.471 (2)	4.0 (5)
C(23)	0.540 (2)	0.2310 (9)	0.187 (2)	4.4 (5)
C(24)	0.759 (2)	0.2686 (7)	0.243 (2)	3.7 (5)
C(25)	0.475 (2)	0.422 (2)	0.462 (4)	8.0 (9)
C(26)	0.688 (2)	0.596 (1)	0.713 (5)	9 (1)

[a] The value marked with an asterisk denotes the isotropically refined atom. The isotropic equivalent thermal parameters of the anisotropically refined atoms are defined as $^4/_3[a^2\beta_{11} + b^2\beta_{22} + c^2\beta_{33} + ab(\cos\gamma)\beta_{12} + ac(\cos\beta)\beta_{13} + bc(\cos\alpha)\beta_{23}]$.

Table IX. Positional and Thermal Parameters and Their Esd's for $[Pt_2(CH_3)_4(fhp)_2(py)_2]\cdot 0.17C_6H_6$[a]

atom	*x*	*y*	*z*	*B*, Å^2
Pt(1)	0.43916 (4)	0.32282 (4)	0.6756 (1)	3.06 (3)
Pt(2)	0.46016 (4)	0.32943 (4)	0.4794 (1)	3.20 (3)
F(1)	0.5179 (6)	0.3800 (6)	0.853 (1)	6.4 (6)
F(2)	0.3935 (5)	0.2510 (6)	0.312 (1)	5.4 (5)
O(1)	0.5150 (5)	0.3166 (6)	0.536 (1)	3.8 (5)
O(2)	0.4283 (5)	0.2541 (6)	0.654 (2)	3.7 (5)
N(1)	0.5143 (6)	0.3471 (7)	0.703 (2)	3.0 (6)
N(2)	0.4113 (8)	0.2505 (7)	0.484 (2)	4.4 (7)
N(3)	0.4231 (7)	0.3046 (7)	0.844 (2)	3.5 (6)
N(4)	0.4894 (7)	0.3294 (6)	0.321 (2)	3.3 (6)
C(1)	0.5346 (9)	0.3321 (9)	0.628 (2)	3.8 (8)
C(2)	0.5831 (9)	0.340 (1)	0.642 (2)	4.8 (9)
C(3)	0.6068 (9)	0.3635 (9)	0.734 (3)	5.1 (9)
C(4)	0.5847 (9)	0.3775 (9)	0.813 (2)	4.5 (9)
C(5)	0.5422 (9)	0.3675 (8)	0.780 (2)	3.9 (8)
C(11)	0.4080 (7)	0.2279 (7)	0.577 (2)	2.2 (7)
C(12)	0.3812 (9)	0.1799 (9)	0.580 (3)	4.4 (7)*
C(13)	0.3582 (9)	0.1551 (9)	0.493 (3)	4.9 (9)
C(14)	0.3605 (9)	0.1774 (9)	0.397 (3)	4.6 (9)
C(15)	0.390 (1)	0.227 (1)	0.403 (3)	7.5 (9)
C(20)	0.3687 (8)	0.298 (1)	0.652 (3)	4.9 (9)
C(21)	0.4477 (9)	0.3885 (8)	0.696 (2)	4.1 (8)
C(22)	0.5076 (8)	0.4015 (8)	0.484 (2)	3.3 (6)*
C(23)	0.4108 (9)	0.3451 (9)	0.422 (3)	5.6 (9)
C(31)	0.403 (1)	0.3200 (9)	0.907 (2)	4.4 (9)
C(32)	0.391 (1)	0.306 (1)	1.006 (3)	7 (1)*
C(33)	0.406 (1)	0.276 (1)	1.047 (3)	7 (1)
C(34)	0.427 (1)	0.256 (1)	0.985 (3)	5 (1)
C(35)	0.437 (1)	0.273 (1)	0.881 (3)	6 (1)
C(41)	0.5039 (9)	0.296 (1)	0.312 (3)	6 (1)
C(42)	0.527 (1)	0.297 (1)	0.212 (3)	6 (1)
C(43)	0.535 (1)	0.329 (1)	0.131 (3)	7 (1)
C(44)	0.522 (1)	0.363 (1)	0.151 (3)	7 (1)
C(45)	0.497 (1)	0.362 (1)	0.245 (3)	5 (1)

[a] Values marked with an asterisk denote isotropically refined atoms. The isotropic equivalent thermal parameters of the anisotropically refined atoms are defined as $^4/_3[a^2\beta_{11} + b^2\beta_{22} + c^2\beta_{33} + ab(\cos\gamma)\beta_{12} + ac(\cos\beta)\beta_{13} + bc(\cos\alpha)\beta_{23}]$.

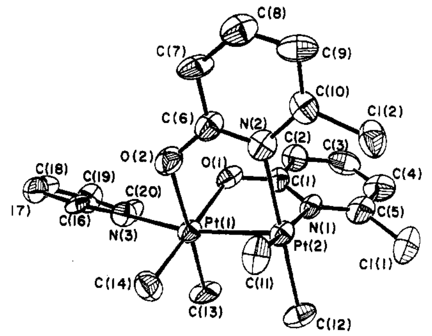

Figure 5. ORTEP view of $[Pt_2(CH_3)_4(chp)_2(py)]$.

with an average Pt–Pt–N$_{ax}$ bond angle of 168.1 [17]°. As in the acetate case, there are two cis methyl groups bonded to each Pt atom. There is a staggered conformation about the metal–metal bond with an average torsional angle of +31 [2]°.

Structure of $[Pt_2(CH_3)_4(fhp)_2(py)_2]$. An ORTEP view is shown in Figure 4. Table IX contains final positional and thermal parameters. Tables VI and VII list some selected bond distances and angles.

The molecular structure consists of a binuclear Pt(III) molecule that has a Pt–Pt bond distance of 2.551 (2) Å. The Pt$_2$ unit is bridged by two fhp ligands that are arranged in a nonpolar manner. Each Pt(III) center has an axially coordinated pyridine molecule with an average Pt–N$_{ax}$ distance of 2.20 [1] Å. The average Pt–N$_{ax}$ bond angle is 167.6 [11]° with the pyridine molecules being bent away from the cis methyl groups. As before, the cis methyl groups in the two equatorial planes sterically interact causing a mean torsion angle of ±31.5 [3]° about the Pt–Pt vector. The average Pt–C bond length is 2.06 [2] Å.

Structure of $[Pt_2(CH_3)_4(chp)_2(py)]$. An ORTEP view of the molecule is shown in Figure 5. Table X contains the final positional and thermal parameters. Tables VI and VII list some selected bond lengths and angles.

The molecular structure comprises a binuclear Pt(III) molecule that has a Pt–Pt bond distance of 2.545 (1) Å. The platinum atoms are bridged by two chp ligands that are arranged in a polar manner with the chlorine atoms effectively blocking one axial site. The other axial site is occupied by a pyridine molecule, strongly coordinated with a Pt–N$_{ax}$ distance of 2.060 (11) Å. As in the carboxylate case, the axial ligand is bent away from the cis methyl groups by approximately 11°. The complex is distorted toward a staggered conformation due to steric interaction between the methyl groups in the equatorial coordination planes, with a mean torsional angle of ±27.2 [1]°. The average Pt–C bond distance is 2.04 [1] Å.

Structure of $[Pt_2(CH_3)_4(mhp)_2(py)]$. An ORTEP view is shown in Figure 6. Table XI contains final positional and thermal parameters. Tables VI and VII list some selected bond distances and angles.

The structure is very similar to that of $[Pt_2(CH_3)_4(chp)_2(py)]$ described above. The mhp ligands bridge the two platinum atoms in a polar manner with the ligand methyl groups blocking one axial site. The Pt–Pt bond distance, which is 2.543 (1) Å, is identical within experimental error with the distance in the analogous chp complex. The axial pyridine molecule is bent away from the cis methyl groups and is very strongly coordinated, with the Pt–N$_{ax}$

Table X. Positional and Thermal Parameters and Their Esd's for $[Pt_2(CH_3)_4(chp)_2(py)]^a$

atom	*x*	*y*	*z*	*B*, Å^2
Pt(1)	−0.29258 (8)	−0.31596 (8)	−0.14218 (6)	2.54 (2)
Pt(2)	−0.11895 (8)	−0.36622 (8)	−0.28941 (6)	2.56 (2)
Cl(1)	−0.1969 (7)	−0.4607 (7)	−0.5355 (4)	4.8 (1)
Cl(2)	0.0727 (7)	−0.1825 (7)	−0.4510 (4)	4.6 (1)
O(1)	−0.396 (1)	−0.192 (1)	−0.250 (1)	3.1 (3)
O(2)	−0.132 (2)	−0.132 (1)	−0.108 (1)	3.8 (3)
N(1)	−0.305 (2)	−0.313 (2)	−0.385 (1)	2.6 (3)
N(2)	−0.041 (2)	−0.142 (2)	−0.271 (1)	3.0 (4)
N(3)	−0.429 (2)	−0.236 (2)	−0.033 (1)	3.2 (4)
C(1)	−0.404 (2)	−0.224 (2)	−0.347 (1)	2.6 (4)
C(2)	−0.510 (2)	−0.169 (2)	−0.406 (2)	3.8 (5)
C(4)	−0.423 (3)	−0.299 (2)	−0.553 (2)	4.2 (5)
C(5)	−0.321 (2)	−0.348 (2)	−0.485 (2)	3.9 (5)
C(6)	−0.056 (2)	−0.070 (2)	−0.183 (2)	3.4 (5)
C(7)	0.007 (2)	0.075 (2)	−0.168 (2)	4.0 (5)
C(8)	0.088 (2)	0.135 (2)	−0.245 (2)	4.5 (6)
C(9)	0.113 (2)	0.064 (2)	−0.338 (2)	4.3 (5)
C(10)	0.049 (2)	−0.075 (2)	−0.343 (1)	3.5 (5)
C(11)	0.070 (2)	−0.403 (2)	−0.209 (2)	3.7 (5)
C(12)	−0.170 (3)	−0.580 (2)	−0.303 (2)	3.9 (5)
C(13)	−0.453 (3)	−0.487 (2)	−0.170 (2)	4.5 (5)
C(14)	−0.196 (3)	−0.433 (2)	−0.038 (2)	4.0 (5)
C(16)	−0.373 (2)	−0.188 (2)	0.057 (1)	3.1 (4)
C(17)	−0.460 (3)	−0.126 (2)	0.127 (2)	4.3 (5)
C(18)	−0.617 (2)	−0.113 (2)	0.105 (2)	4.1 (5)
C(19)	−0.672 (2)	−0.167 (2)	0.013 (2)	3.9 (5)
C(3)	−0.522 (3)	−0.209 (2)	−0.509 (2)	4.3 (5)
C(20)	−0.585 (2)	−0.231 (2)	−0.057 (2)	3.9 (5)

[a] The isotropic equivalent thermal parameters of the anisotropically refined atoms are defined as $^4/_3[a^2\beta_{11} + b^2\beta_{22} + c^2\beta_{33} + ab(\cos\gamma)\beta_{12} + ac(\cos\beta)\beta_{13} + bc(\cos\alpha)\beta_{23}]$.

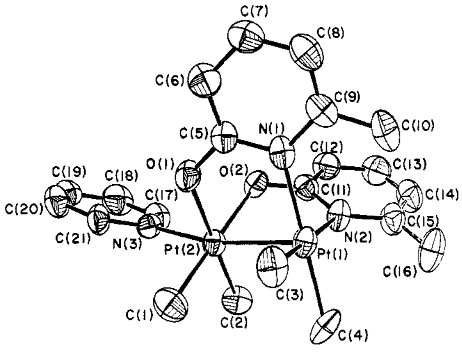

Figure 6. ORTEP view of $[Pt_2(CH_3)_4(mhp)_2(py)]$.

distance being 2.030 (8) Å. There is a mean torsional angle of ±31 [1]° about the Pt–Pt vector due to steric interaction between the methyl groups in the two equatorial coordination planes. The average Pt–C bond length is 2.051 [10] Å.

Discussion

The compound $[Pt_2(CH_3)_4((C_2H_5)_2S)_2]$ (**1**) has proved to be a generally useful starting material for the synthesis of a class of diplatinum(III) complexes of the general type shown schematically as I. Vrieze had previously shown that the bidentate

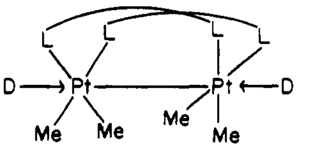

I

bridging ligand, LL, could be practically any carboxylate anion (and also, incidentally, that comparable chemistry occurs with phenyl in place of methyl). Our present work generalizes this chemistry further by showing that the LL ligands may be of the 2-oxypyridine (α-pyrazolato) type as well.

We have confirmed the type of structure proposed for **1** by Vrieze and can now supply quantitative details. It is, indeed, a $(C_2H_5)_2S$-bridged dimethylplatinum(II) compound, involving distorted square-planar coordination of the Pt(II) centers and no significant Pt–Pt interaction (Pt–Pt = 3.610 (1) Å). It is readily oxidized, not only by AgO_2CR compounds, but also by the Ag(hp), Ag(mhp), Ag(chp), and Ag(fhp) compounds.

Table XI. Positional and Thermal Parameters and Their Esd's for $[Pt_2(CH_3)_4(mhp)_2(py)]^a$

atom	*x*	*y*	*z*	*B*, Å^2
Pt(1)	0.04844 (6)	0.12717 (5)	0.31520 (3)	3.17 (1)
Pt(2)	0.16389 (6)	0.31305 (5)	0.20518 (3)	2.782 (9)
O(1)	0.027 (1)	0.134 (1)	0.1198 (5)	3.7 (2)
O(2)	−0.067 (1)	0.3960 (9)	0.2268 (5)	3.2 (2)
N(1)	−0.150 (1)	0.037 (1)	0.2229 (7)	3.2 (2)
N(2)	−0.088 (1)	0.307 (1)	0.3586 (7)	3.4 (2)
N(3)	0.204 (1)	0.451 (1)	0.1078 (6)	2.9 (2)
C(1)	0.388 (2)	0.238 (2)	0.185 (1)	4.8 (4)
C(2)	0.289 (2)	0.491 (1)	0.2856 (9)	3.7 (3)
C(3)	0.164 (2)	−0.057 (1)	0.275 (1)	4.3 (3)
C(4)	0.243 (2)	0.190 (2)	0.4014 (8)	4.6 (3)
C(5)	−0.115 (1)	0.049 (1)	0.1394 (8)	3.2 (3)
C(6)	−0.227 (2)	−0.026 (2)	0.076 (1)	4.3 (3)
C(7)	−0.382 (2)	−0.111 (1)	0.099 (1)	4.3 (3)
C(8)	−0.419 (2)	−0.124 (2)	0.184 (1)	4.5 (3)
C(9)	−0.302 (1)	−0.054 (1)	0.2433 (9)	3.6 (3)
C(10)	−0.334 (2)	−0.067 (2)	0.337 (1)	5.1 (4)
C(11)	−0.131 (1)	0.402 (1)	0.3007 (8)	3.2 (3)
C(12)	−0.237 (2)	0.508 (2)	0.3226 (9)	3.9 (3)
C(13)	−0.303 (2)	0.518 (2)	0.402 (1)	4.6 (3)
C(14)	−0.263 (2)	0.421 (2)	0.4590 (9)	4.5 (3)
C(15)	−0.157 (2)	0.317 (2)	0.4389 (9)	4.1 (3)
C(16)	−0.113 (2)	0.211 (2)	0.502 (1)	5.6 (4)
C(17)	0.162 (2)	0.597 (1)	0.1151 (9)	3.7 (3)
C(18)	0.167 (2)	0.687 (2)	0.046 (1)	5.0 (4)
C(19)	0.222 (2)	0.631 (2)	−0.0305 (9)	4.0 (3)
C(20)	0.264 (2)	0.485 (2)	−0.0365 (9)	4.3 (3)
C(21)	0.256 (2)	0.400 (1)	0.0336 (8)	3.6 (3)

[a] The isotropic equivalent thermal parameters of the anisotropically refined atoms are defined as $^4/_3[a^2\beta_{11} + b^2\beta_{22} + c^2\beta_{33} + ab(\cos\gamma)\beta_{12} + ac(\cos\beta)\beta_{13} + bc(\cos\alpha)\beta_{23}]$.

In all cases, the $(C_2H_5)_2S$ molecules tend to be retained as axial ligands in the initial products, but they are easily displaced by other donors. In all of our work we have displaced the $(C_2H_5)_2S$ and introduced pyridine as the axial donor ligand.

We began our work by examining a carboxylato-bridged compound with axial pyridine ligands, **2**, which should be the closest carboxylato analogue to the other compounds we have studied and also very similar to the one compound previously studied[8] by X-ray crystallography, $[Pt_2(CH_3)_4(O_2CCF_3)_2(4\text{-}CH_3C_5H_4N)_2]$. The overall similarity of the two carboxyl compounds is close. The only difference that may be chemically significant is in the Pt–Pt distances, which are 2.529 (1) Å for the acetate and 2.557 (1) Å for the trifluoroacetate. The difference is about 20 times the esd and is thus presumed to be statistically real. It is also in a direction that seems chemically reasonable. With the less electron-withdrawing ligands, a somewhat lower effective charge on the metal atoms would be expected and this in turn would lead to better Pt–Pt overlap and hence a stronger bond. The size of the experimental errors in all other distances (plus the fact that the lack of any crystallographic symmetry for the trifluoroacetate compound allows several large discrepancies; e.g., the two Pt–N_{ax} distances are 2.09 (2) and 2.17 (2) Å), means that there are no other differences in distances between the two molecules that have significance. The more important angles are also very similar. Thus, the degree of nonlinearity of the Pt–Pt–N chains as well as the torsion angles about the Pt–Pt bonds are virtually the same in the two cases.

The four compounds containing the hydroxypyridinate ligands, hp$^-$, mhp$^-$, chp$^-$, and fhp$^-$, display both similarities to their carboxylato analogues and important differences. Comparisons among all five of these compounds are facilitated by the tabulation of average values of bond lengths and angles presented in Tables VI and VII. We begin with compounds **3** and **4**, which most closely resemble the carboxylato compounds.

Compounds **3** and **4** have many features that are similar to those of the carboxylato complexes. Both compounds have two cis methyl groups bonded to each platinum center. In addition, as in the carboxylato compounds, there is a substantial torsion about the Pt–Pt bond due to steric interaction between the two equatorial coordination planes. The compounds also have two axially coordinated pyridine molecules that are bent away from the methyl groups in a similar manner. The Pt–C and Pt–N$_{ax}$ bond distances are identical within experimental error to those present in the carboxylato compounds. The metal–metal distances are virtually identical and are intermediate between the Pt–Pt distances present in the two structurally characterized carboxylate compounds. Additionally, many of the more important bond angles are similar to those present in the carboxylato analogues. The primary difference between the carboxylate and hydroxypyridinate compounds lies with the bridging ligands. The hydroxypyridinate compounds, **3** and **4**, have bridging ligands with relatively small substituents in the 6-positions. In both cases, the two platinum atoms are bridged in a nonpolar manner by two oppositely directed hydroxypyridinate ligands. This type of asymmetry is not possible in the analogous carboxylato compounds. The torsion about the metal–metal bond, due to the steric interaction of the methyl groups, forces the bridging ligands to distort from planarity in both the carboxylate and hydroxypyridinate cases. Compounds **3** and **4** have nearly identical C–Pt–Pt–C and O–Pt–Pt–N mean torsional angles and both torsional angles are larger than those present in the carboxylato compounds. Thus, despite the asymmetry introduced by the hydroxypyridinate ligands and the larger torsional angles, compounds **3** and **4** are remarkably similar to their carboxylato analogues.

Compounds **5** and **6**, like compounds **3** and **4**, have several features that are similar to those of the carboxylato complexes. However, several important differences are observed between compounds **5** and **6** and both the carboxylato and the other hydroxypyridine compounds. As before, both compounds have two cis methyl groups bonded to each platinum center and the resultant torsional twist about the metal–metal bond, due to the steric interaction between the two equatorial coordination planes, is present. In addition, the mean Pt–C bond distances as well as several of the important bond angles are similar to those in the other compounds. However, compounds **5** and **6** have hydroxypyridinate bridging ligands with relatively large substituents in the 6-positions, and the size of these substituents has a substantial effect on the coordination geometry of the resultant compounds. In both cases, the two compounds are bridged in a polar manner by the hydroxypyridinate ligands.

The polar structures of **5** and **6** can be contrasted to the head-to-tail structures of compounds **3** and **4**. The large ring substituents present in compounds **5** and **6** effectively block one axial site preventing the binding of a second axial ligand, whereas in the other hydroxypyridinate compounds the small ring substituents have little effect on the axial coordination. Although compounds **5** and **6** have different bridging ligands and possess a different coordination geometry, the metal–ligand bond distances as well as the L–M–M–L torsional angles are similar to those in the other hydroxypyridinate compounds.

The metal–metal distances are virtually identical and are only slightly shorter than those in compounds **3** and **4**. As before, the metal–metal distances are intermediate between those of the two structurally characterized carboxylate compounds. One very important difference between compounds **5** and **6** and the rest of the compounds is the presence of very short Pt–N$_{ax}$ bond distances. The Pt–N$_{ax}$ bond distances in compounds **5** and **6** are ca. 0.16 Å shorter than the axial bond distances present in the other compounds.

This set of compounds, **3–6**, evidently exhibits a type of behavior similar to that in other $M_2(xhp)_4X_n$ species,[9-13] where stereochemistry controls the structure and composition in a way that depends on the bulk of the 6-substituent, x, in the xhp$^-$ ligand. In the present compounds, when x is small, namely H or F, the xhp ligands can adopt the head-to-tail (nonpolar) arrangement and still leave both axial positions sufficiently unencumbered to allow a pyridine molecule to be coordinated at each end. However, with the larger x groups, Cl or CH_3, it is probable that with even one of these projecting into the axial region that position would be relatively inaccessible to an axial ligand. Thus, with the chp$^-$ or mhp$^-$ ligands in a nonpolar, head-to-tail arrangement, no satisfactory axial ligation could occur. However, with the polar arrangement, one axial position is left free for the formation of one strong axial bond.

The polar arrangement is not, in itself, disfavored by the presence of the Cl or CH_3 substituents since there are only two of them and the torsional twist that is favored by other factors anyway helps them to avoid close contact. In this respect these molecules differ from the type with four bridging xhp ligands, where it is difficult to accommodate four Cl substituents at one end[9,11] and apparently impossible to accommodate four methyl substituents at one end.[10]

It may be noted that in the molecule of compound **4** we have the first case where bridging fhp$^-$ ligands have adopted a nonpolar arrangement. In all cases where there have been four of them, the polar arrangement has been found.[12,13] The reason for this appears to be that in a molecule where there are only two head-to-tail fhp$^-$ ligands (e.g., **4**) both axial positions remain fairly accessible, so that the $[Pt_2(CH_3)_4(fhp)_2(py)_2]$ molecule is able to compete with, and actually win out over, the molecule with only one axial ligand that would result if there were a polar arrangement of fhp ligands leading to a blockage of one end. In the case of a $M_2(fhp)_4$ species, the 2:2 (nonpolar) arrangement would block both ends so that the polar arrangement, which leaves one axial position free without creating excessive crowding at the other end, is favored.[12,13]

Finally, the $[Pt_2(CH_3)_4(xhp)_2(py)_2]$ molecules (x = H, F) can be directly compared with the various $[Pt(NH_3)_4(hp)_2LL']^{n+}$ species, where $L = L' = NO_3^-$ and $n = 2$, $L = NO_3^-$, $L' = H_2O$ and $n = 3$, $L = L' = Cl^-$ and $n = 2$, and $L = NO_2^-$, $L' = NO_3^-$, and $n = 2$, that have been described by Lippard and co-workers.[14-16] In these compounds the Pt–Pt distances are in the range 2.539 (1)–2.575 (1) Å, which is very similar to the range found here, despite the different distribution of charge. Also, these tetraammine species have internal torsion angles comparable to those found here.

We are now developing the chemistry of these new compounds, as well as that of some of the previously known ones,[6,7,14-16] along lines in which the Pt–Pt bonds are conserved, and future publications will present these results.

Acknowledgment. We are grateful to the National Science Foundation for support.

Registry No. **1**, 62343-09-3; **2**, 100351-34-6; **3**, 100351-35-7; **4**, 100351-36-8; **5**, 100430-64-6; **6**, 100351-37-9; *cis*-$PtCl_2((C_2H_5)_2S)_2$, 15442-57-6; $Ag(O_2CCH_3)$, 563-63-3; Ag(hp), 22918-00-9; Ag(fhp), 100366-72-1; Ag(chp), 100366-73-2; Ag(mhp), 93355-10-3; Pt, 7440-06-4.

Supplementary Material Available: Tables of bond distances and bond angles, anisotropic thermal parameters, torsional angles (compounds **2–6**), and observed and calculated structure factors for compounds **1–6** (86 pages). Ordering information is given on any current masthead page.

---

(9) Chakravarty, A. R.; Cotton, F. A.; Tocher, D. A. *Inorg. Chem.* **1985**, *24*, 1263.

(10) Chakravarty, A. R.; Cotton, F. A.; Tocher, D. A. *Inorg. Chem.* **1985**, *24*, 2857.

(11) Cotton, F. A.; Dunbar, K. R.; Matusz, M. *J. Am. Chem. Soc.*, in press.

(12) Cotton, F. A.; Han, S.; Wang, W. *Inorg. Chem.* **1984**, *23*, 4762.

(13) Chakravarty, A. R.; Cotton, F. A.; Schwotzer, W. *Polyhedron*, in press.

(14) Hollis, L. S.; Lippard, S. J. *J. Am. Chem. Soc.* **1981**, *103*, 6761.

(15) Hollis, L. S.; Lippard, S. J. *Inorg. Chem.* **1982**, 21, 2116.

(16) Hollis, L. S.; Roberts, M. M.; Lippard, S. J. *Inorg. Chem.* **1983**, *22*, 3637.